Julio A. Deiber[1]
Marta B. Peirotti[1]
Maria V. Piaggio[2]

[1]Instituto de Desarrollo Tecnológico para la Industria Química (INTEC), Universidad Nacional del Litoral (UNL), Consejo Nacional de Investigaciones Científicas y Técnicas (CONICET), Santa Fe, Argentina
[2]Cátedra de Bioquímica Básica de Macromoléculas, Facultad de Bioquímica y Ciencias Biológicas, UNL, Santa Fe, Argentina

Received August 21, 2015
Revised November 10, 2015
Accepted December 16, 2015

Research Article

Charge regulation phenomenon predicted from the modeling of polypeptide electrophoretic mobilities as a relevant mechanism of amyloid-beta peptide oligomerization

Electrophoretic mobilities of amyloid-beta (1-40) and (1-42) peptides and their aggregates are modeled to study the amyloidogenic pathway associated with Alzheimer´s Disease. The near molecule pH generated by the intraparticle charge regulation phenomenon during the oligomerization of amyloid-beta (1-40) and (1-42) peptides is evaluated and discussed as a relevant mechanism supporting the "amyloid cascade hypothesis" proposed in the literature. A theoretical framework associated with the oligomerization of amyloid-beta peptides including simple scaling laws and the consideration of electrokinetic and hydrodynamic global properties of oligomers is presented. The central finding is the explanation of the near molecule pH change toward the pI when the oligomerization number increases. These results allow one to rationalize consecutive physical stages that validate the amyloid cascade hypothesis. Concluding remarks involving mainly the effects of pair and intraparticle charge regulation phenomena on the amyloidogenic pathway with some suggestions for future research are provided.

Keywords:
Amyloid-beta peptides / Amyloid cascade hypothesis / Charge regulation phenomenon / Electrophoretic mobility / Peptide oligomerization
DOI 10.1002/elps.201500391

Additional supporting information may be found in the online version of this article at the publisher's web-site

1 Introduction

At present CZE is the suited analytical method [1–6] required to characterize electrokinetic and hydrodynamic global properties of polyampholyte-polypeptide hetero-chains through the modeling of their effective electrophoretic mobilities in BGEs with well-defined pH, ionic strength I, temperature T, electrical permittivity ε and viscosity η_s as described for instance in refs. 7–33. In this regard, proteins and peptides of biological systems may be studied in different BGEs not only to separate them efficiently but also to elucidate, for example, relevant bioprocesses found in human pathologies. In fact the evaluations of electrokinetic and hydrodynamic global properties of these polypeptide chains are unavoidable steps toward the understanding of key associated biophysical mechanisms. Within this framework a specific case is Alzheimer´s Disease (AD), in which one of the most probable causes of neuronal activity loss is the toxicity produced by the formation of soluble amyloid-beta (Aβ) peptides aggregates mainly from Aβ(1-42) and Aβ(1-40). The oligomerization of Aβ peptides seems to be a consequence of an imbalance between their production and clearance, where the relative concentration between apoliproteins E3 and E4 may be crucial [34]. The process transforming Aβ peptides (monomers) into higher soluble oligomers and fibril formations generated the "amyloid cascade hypothesis" associated with AD [35–37]. The result is an increase in Aβ peptide soluble oligomers, intermediates, and fibrils with a progressive formation of extracellular amyloid plaques, where addition

Correspondence: Dr. Julio A. Deiber, Instituto de Desarrollo Tecnológico para la Industria Química (INTEC), Universidad Nacional del Litoral (UNL), Consejo Nacional de Investigaciones Científicas y Técnicas (CONICET), Güemes 3450, 3000, Santa Fe, Argentina
E-mail: treoflu@santafe-conicet.gov.ar
Fax: +54-(0)342-4550944

Abbreviations: AAS, amino acid sequence; **Aβ**, amyloid-beta; **AD**, Alzheimer's Disease; **ICPR**, ion convection-polarization-relaxation; **IPCR**, intraparticle charge regulation; **PLLCEM**, Perturbed Linderstrom-Lang Capillary Electrophoresis Model; **PPCR**, pair particle charge regulation

of new aggregates occurs. In this context the causes promoting Aβ peptides aggregation need to be elucidated, and one may conclude that the principal mechanisms yielding extracellular plaques are not fully understood yet. The interest of the present work is precisely the study of the Aβ peptide amyloidogenic pathway through the modeling of effective electrophoretic mobilities of oligomers as measured via the CZE method.

The biophysical mechanisms leading to Aβ(1-40) and Aβ(1-42) aggregations may be targeted from two basic scales [31, 32]. One considers details of peptide primary configurations and structures described by the amino acid sequence (AAS) and the physicochemical characteristics of each type of amino acid residue ([38-40] and citations therein), while the other is concerned with peptide chain global properties and conformations associated with hydrodynamic and electrokinetic effects enhancing peptide aggregation [31, 32]. In the consideration of this scale, CZE methods may assist one significantly to understand some of the basic mechanisms of Aβ peptide aggregation at different incubation times by providing particle migration times associated with the detection of monomer and soluble oligomers [41–50].

This work presents the evaluation of global properties of the Aβ(1-40) and Aβ(1-42) peptides (designated here monomers) having a number $N_1 = 40$ and 42 of amino acid residues, respectively, through the modeling of their effective electrophoretic mobilities obtained via CZE-UV as provided in ref. 46. These evaluations are then required to study Aβ(1-40) and Aβ(1-42) soluble oligomers with a given oligomerization number $k>1$ yielding a hydrodynamic particle with a number of amino acid residues $N_k = kN_1$. In this framework, our previous results presented the propensity to aggregation of Aβ(1-40) and Aβ(1-42) estimated by using their electrokinetic and hydrodynamic global properties and established kinetic theories of Brownian aggregation [31, 32, 51, 52]. For these purposes the Perturbed Linderstrøm-Lang Capillary Electrophoresis Model (PLL-CEM) [8, 12, 13, 15, 17, 18, 20, 22, 25, 28, 31, 32] was used by introducing appropriate modifications allowing us to consider the amyloidogenic pathway. This model's applicability to polyampholyte-polypeptide chains has been presented and discussed in details in the Supporting Information of refs. 31, 32 and citations therein. Thus in our work [31] Aβ(1-37) to Aβ(1-40) and Aβ(1-42) were characterized through the modeling of their effective electrophoretic mobilities determined via CZE. Then the resulting electrokinetic and hydrodynamic global properties were used to evaluate amyloid-beta peptide propensities to aggregation through pair particles interaction potentials and Brownian kinetic theories. Peptide aggregation mechanisms of Aβ(1-40) and Aβ(1-42) were described through the interplay among hydration, electrostatic and dispersion forces, mainly in what concerns with the coupling between particle hydration and the near molecule pH designated pH* (see a physical explanation of pH* in the Supporting Information). It was also shown that Aβ(1-40) and Aβ(1-42) formed soluble oligomers, mainly of order 2 and 4 after an incubation of 48 hours at pH 10, $I = 100$ mM and 25ºC. Typical values of the slow kinetic constant in this protocol were $k_s = 5.4\ 10^{-7}$ and $2.1\ 10^{-6}$ ($M^{-1}\ s^{-1}$) for Aβ(1-40) and Aβ(1-42), respectively. Here k_s is expressed via molar concentration instead of number concentration [31] as a more practical unit. Following, we studied [32] the propensity to aggregation of the Aβ(12-28) peptide fragment as monomer and dimer at low pH 2.9 through the modeling of diffusion coefficients reported in ref. 53 and calculated effective electrophoretic mobilities [32]. The resulting electrokinetic and hydrodynamic global properties were employed to evaluate the amyloid-beta (12-28) peptide fragment propensity to dimerization. This theoretical analysis demonstrated that peptide aggregation was a concentration-dependent process, where both pair particle (PPCR) and intraparticle (IPCR) charge regulation phenomena became relevant [31, 32] enhancing a shift of the near molecule pH toward the peptide pI. It was shown that the modeling of the effective electrophoretic mobility of the amyloid-beta (12-28) peptide fragment was crucial to understand the nucleating effect of the hydrophobic region LVFFA in the amyloidogenic pathway, with an enhancement at a critical value of peptide molar fraction. Therefore to provide a closure to our previous studies, here we extend our conclusions [31, 32] to study the effect of the near molecule pH on the oligomerization of Aβ(1-40) and Aβ(1-42) peptides through the modeling of their electrophoretic mobilities.

In this work, Section 2 describes briefly the CZE protocol used in ref. 46 to obtain the experimental electrophoretic mobility values used in the present study of the amyloidogenic pathway. Section 2.2 presents a theoretical framework associated with the oligomerization of Aβ peptides including simple scaling laws useful to analyze the electrokinetic and hydrodynamic global properties of peptide oligomers. Section 3 discusses the calculation of the near molecule pH changes toward the pI with increasing oligomerization numbers in the amyloidogenic pathway, thus allowing us to present then a rationale of possible consecutive physical stages of the amyloid cascade hypothesis. Also an approximate analysis to consider the complex ion convection-polarization-relaxation (ICPR) phenomenon present in the electrophoresis of particles with high electrokinetic (zeta) potentials is included [23, 52, 54–58]. Finally, Section 4 provides concluding remarks and suggestions for future research.

2 Materials and methods

2.1 CZE protocol and electrophoretic mobilities of Aβ peptide monomer and oligomers

The experimental electrophoretic mobility values of Aβ peptides and their oligomers used here were reported in ref. 46 as obtained from a CZE-UV experimental set up. The running electrophoretic buffer was Tris 10 mM at pH 7.79 with an approximate ionic strength $I = 6$ mM at 20ºC. Peptide concentrations were less than 25 μM to assure

solubility. This experimental work was able to differentiate Aβ monomer, oligomers and mature fibrils. The experimental electrophoretic mobilities of Aβ(1-40) and Aβ(1-42) peptide monomers reported were $\mu_{p1}^{exp} = -1.082\,10^{-8}$ m^2/V s and $-1.072\,10^{-8}$ m^2/V s, respectively. Since the Aβ(1-40) was previously incubated in PBS at pH 7.4 and 37°C during 7 days (see details in refs. 45, 46) the CZE electropherogram also presented a second peak of intermediate oligomers (k>1) with $\mu_{pk}^{exp} = -2.39\,10^{-8}$ m^2/V s. On the other hand the Aβ(1-42) without incubation time also presented a second peak associated with the electrophoretic mobilities of oligomers having $\mu_{pk}^{exp} = -2.29\,10^{-8}$ m^2/V s. Further, Picou et al. [46] showed via transmission electron microscopy that in the second peaks of the Aβ(1-40) and Aβ(1-42) electropherograms soluble aggregates were present. In this regard, previous experimental works indicated that although the oligomerization process of monomer Aβ peptides could be accelerated depending relatively on the type of solvent used during the sample pretreatment [49, 59], the resulting oligomers (k>1) had almost the same effective electrophoretic mobility for fixed sample pretreatment and CZE protocol (different oligomerization numbers yielded quite equal migration times) [42]. This result was clearly reflected in the difficulty found to separate mixtures of oligomers generated at different sample incubation times as it was discussed in the literature [42, 45, 46, 49, 50]. These experimental facts certainly involve subtle phenomenological mechanisms to be elucidated, which may provide some explanations associated with the oligomerization process. Thus it will be shown that the separation of the monomer from the corresponding oligomers is crucial to analyze the approximate scaling laws discussed in Section 2.2.2. These considerations justify here the use of the experimental results provided in ref. 46, where the balanced mixture of trifluoroacetic acid and hexafluoroisopropanol solvents used for sample pretreatment was appropriate to separate monomer from oligomers at the indicated CZE protocol.

2.2 Theoretical analyses

2.2.1 The amyloidogenic pathway and stoichiometry

The AAS of the Aβ(1-42) is DAEFRHDSGYEVHHQKLVFFAEDVGSNKGAIIGLMVGGVVIA. In the AAS of Aβ(1-40) the amino acid residues I(41) and A(42) are not present. In general the oligomerization of peptide chains is a concentration-dependent process that may be visualized from different thermodynamic and kinetic theories [31, 32, 53]. Here we study the oligomerization of Aβ peptides forming a mixture of a monomer (k = 1) and its oligomers (k > 1) which are considered as species having oligomerization number k = 1, 2, 3 . . . K in the BGE, where 1, 2, 3 . . . K stand for monomer, dimer, trimer to K-mer, respectively. Throughout the text subscript k is used to indicate that a property or parameter of the model is evaluated at the oligomerization number k (see also the list of symbols in Supporting Information). The oligomerization of Aβ peptides are soluble aggregates where covalent bonds do not occur and the amino and carboxylic terminal groups of the monomer chains are preserved in the resulting oligomers.

2.2.2 Electrokinetic and hydrodynamic global properties of monomer and oligomers

Based on our previous works [28,31,32] monomers (k = 1) and oligomers (k > 1) of Aβ peptides may be described through a set of electrokinetic and hydrodynamic global properties as follows (see list of symbols in Supporting Information): effective $Z_k = Z_{+k} - |Z_{-k}|$, positive Z_{+k}, negative Z_{-k} and total Z_{Tk} charge numbers, approximate hydration number H_k (number of water molecules per monomer or k-oligomer calculated through the hydration function in refs. 15, 18) or particle hydration δ_k (gram of water/gram per monomer or k-oligomer), particle size estimated via the equivalent Stokes hydrodynamic radius a_{Hk}, compact radius a_{ck} accounting the peptide mass only, friction ratio Ω_k (also designated particle asphericity) where both the stick and slip conditions between fluid and hydrated particle may be considered [28], near molecule pH designated pH_k^* due to both IPCR and PPCR phenomena [31, 32]. In addition the hydration number is $H_k = H_{ok} + H_{dk}$ [18, 60], where H_{ok} is the number of water molecules captured by amino acid residues of the AAS [15], while H_{dk} is the number of water molecules due to the degree of water occluded or released by either monomer or k-oligomer [31, 32, 60]. Since a k-oligomer is composed of k monomer chains, some simple relationships between them may be established by observing that the number of i-type of amino acid residue in the k aggregate is $n_{ik} = k\, n_{i1}$, which are also classified as weak ionizing, polar and nonpolar amino acid residues [15]. Then the total number of amino acid residues per aggregate is $N_k = \sum_i n_{ik}$, the aggregate molar mass is $M_k = k\, M_1$, where the monomer molar mass is $M_1 = \sum_i n_{i1} M_i + 18$, and the i-type of amino acid residue molar mass is M_i. It is also clear that $\delta_k = H_k 18/M_k$.

The peptide characterization also requires the evaluation of pH_k^* through the following expression [8, 13, 15]:

$$pH_k^* = pH + e\zeta_k/\ln(10)k_B T \quad (1)$$

where k_B is Boltzmann constant, e is the elementary charge and ζ_k is the zeta potential. As long as the hypotheses of the PLLCEM apply [8] the zeta potential may be estimated from $\zeta_k \approx eZ_k/4\pi\,\varepsilon\, a_{Hk}(1 + \kappa\, a_{Hk})$ where $Z_k = \sum_i n_{ik} Z_{ik}$is the effective charge number for k = 1 to K when i sums only the i-types of weak ionizing amino acid residues (Arg, Lys, His, Asp, Glu, Tyr and Cys) including terminal amino and carboxyl ionizing groups. Here $\kappa = (2Ie^2 N_A 10^3/\varepsilon\, k_B T)^{1/2}$ is the Debye-Hückel parameter, $Z_{ik} = \pm 1/(1 + 10^{\mp(pK_{ir} - pH_k^*)})$ is evaluated at pH_k^* and also involves the reference pK designated pK_{ir} [15] of the i-type of weak ionizing amino acid residues, and N_A is Avogadro constant. These expressions show clearly that in order to define the electrostatic state of a polyampholyte chain one needs the effective charge number and the equivalent Stokes hydrodynamic radius

which are implicit functions of pH_k^*. In addition the hydrodynamic volume ($4\pi a_{Hk}^3/3$) of monomers ($k = 1$) and oligomers ($k > 1$) is equivalent to the sum of the whole compact peptide volume plus the hydration volume giving $a_{Hk} = (3M_k(v_p + \delta_k v_w)/4\pi N_A)^{1/3}$, where v_p and v_w are peptide and water specific volumes, respectively [12]. From the above expressions it is clear that for any k-oligomer, one can define a similar set of hydrodynamic and electrokinetic global properties as those of proteins and peptides reported in our previous works [28, 31, 32].

In this framework the chain-solvent friction coefficient of monomer and oligomers is $f_k = 6\pi\eta_s a_o N_k^{g_{fk}}$ for $k = 1$ to K [20, 22, 25], where the fractal friction dimension g_{fk} is in the range $1/3 < g_{fk} < 1$ involving the collapsed globule and the free draining chain at the extremes, respectively, and a_o is the average radius of amino acid residues in the AAS [18].

The definition of particle asphericity $\Omega_k = 6\pi\eta_s a_{Hk}/f_k$ is the relevant information sensitive to hydration, size and shape of peptides visualized as different types of hydrodynamic particles [20,25]. Also concerning the physical interplay between particle shape and hydration as a function of pH_k^* and following our previous works [18, 20, 22, 31, 60] one may consider the minimum δ_k sampled by the particle ($H_{dk} = 0$ and $\Omega_k < 1$) and the maximum δ_k physically admissible ($H_{dk} > 0$ and $\Omega_k = 1$) where in both cases the stick boundary condition between particle and solvent is satisfied. Partial BGE slip on particle surface applies when $\Omega_k > 1$ with $H_{dk} = 0$ for both spherical and aspherical hydrated particles [28,31,60]. In this case $H_{dk} < 0$ is required to obtain BGE stick on particle surface with $\Omega_k = 1$ as far as $a_{Hk} \geq a_{ck}$ can be satisfied.

Since CZE data concerning the amyloidogenic pathway of soluble aggregates show a second peak in the electropherogram involving oligomers having almost the same μ_{pk}^{exp} apart from the monomer peak (Section 2), these phenomenological aspects require further explanation concerning the change of the pH_k^* in the aggregation of peptides. It is clear that when the charge regulation phenomenon is considered, one expects changes of the electrokinetic and hydrodynamic global properties to keep consistency with experimental facts. We may anticipate here that the consequences of keeping almost the same electrophoretic mobility values of soluble aggregates as k increases, implies systematic shifts of pH_k^* toward the pI = 5.44 (this pI is the same for any k value). Also at an appropriate concentration the propensity to aggregation is enhanced due to the PPCR phenomenon for any k value as inferred when one applies to oligomers the results reported in ref [32] for a dimer formation from two monomer fragments.

Before ending this section, it is interesting to analyze the zeta potential for the ideal case in which the charge regulation phenomenon is assumed small ($pH_k^* \approx pH$) and hence the three additional relations apply for the k-oligomer: $Z_k \approx k Z_1$, $H_k \approx k H_1$ and $a_{Hk} \approx k^{1/3} a_{H1}$. These relations readily yield $\zeta_k \approx \zeta_1(1 + \kappa a_{H1})\, k/(k^{1/3} + \kappa a_{H1} k^{2/3})$ for any oligomer indicating that the zeta potential becomes higher as the oligomerization number increases, satisfying the asymptote $\zeta_k \propto k^{1/3}$. The relevant result from these approximate expressions is that the oligomerization process affects the aggregate zeta potential and the pH_k^* also changes with k indicating that $pH_k^* \approx pH$ is a rather gross approximation. In fact, for a bulk pH around 7.3 to 7.4 of the cerebrospinal fluid and plasma, respectively, and knowing that both Aβ(1-40) and Aβ (1-42) have pI = 5.44 [31, 32] it is clear that $\zeta_1 < 0$, and still within similar hypotheses one gets from Eq. (1),

$$pH_k^* \approx pH - e\,|\zeta_1|\,(1 + \kappa a_{H1})k/(k^{1/3} + \kappa a_{H1} k^{2/3})/\ln(10) k_B T \tag{2}$$

Equation (2) shows that $pH_k^* \to pI$ when k increases and consequently $Z_k \to 0$. The same pH_k^* tendency applies when $pH < pI$ and $\zeta_1 > 0$ as shown for proteins and peptides in refs. 26, 60. Thus oligomers can start to collapse together at a critical k value. Concomitantly a critical monomer concentration is also required because the PPCR is a concentration-dependent phenomenon as described previously [32]. Section 2.2.3 demonstrates that the approximate scaling laws presented above provide a rapid visualization of main electrokinetic results (Section 3) obtained through numerical solutions of effective electrophoretic mobility models considering both the IPCR phenomenon due to the oligomerization process, and the ICPR phenomenon at high zeta potentials.

2.2.3 Calculations of monomer and oligomer global properties

The calculations of peptides global properties are carried out in the framework of the equivalent spherical particle model for aspherical particles [12], where the zeta potential of the actual particle is assumed similar to that found in the equivalent spherical particle with the same hydrodynamic volume. Therefore, for the range of low zeta potentials, global properties may be evaluated through the PLLCEM valid for polypeptide chains. In this regard, to visualize better the basic procedure, the use of dimensionless parameters involving the electrophoretic mobility of these particles is appropriate as reported in [18, 20, 25, 52, 54]. Thus functions $Y_k = Y_k(X_k, P_k)$ of the dimensionless electrophoretic mobility $Y_k = 3\mu_{pk}^{exp}\eta_s e/2\Omega_k \varepsilon k_B T$, zeta potential $X_k = e\zeta_k/k_B T$ and Stokes hydrodynamic radius $P_k = \kappa a_{Hk}$ for an oligomerization number k show that for rather small particles ($P_k < 3$), the Hückel branch is obtained from Henry´s theory when the dimensionless zeta potential satisfies $X_k < 2.5$. These results allowed us to consider simply the effects of particle asphericity $\Omega_k \neq 1$ in the coordinate Y_k [18,20]. On the other hand when the dimensionless zeta potential becomes high ($X_k > 2.5$), the ICPR phenomenon is important in CZE [23, 54–58]. For these cases we carried out an approximate correction of basic calculations by using previous numerical results of functions $Y_k = Y_k(X_k, P_k)$ within the full range of X_k (see calculation steps in Supporting Information). Thus dimensionless parameters involving the electrophoretic mobility of these particles were used by observing that Y_k and P_k could be estimated directly from μ_{pk}^{exp} value, and also from both asphericity Ω_k and hydrodynamic radius a_{Hk} provided by the PLLCEM for a first iteration.

Here we assumed that the particle asphericity did not change with the appearance of ICPR. These considerations allowed us to obtain X_k, and hence ζ_k, from the numerically computed parametric curves $Y_k = Y_k(X_k, P_k)$ reported in refs. 52, 54. Therefore when $X_k > 2.5$ the ζ_k value calculated from the PLLCEM differed from that provided by numerical curves indicating that ICPR was significant around the translating particle at the k level of oligomerization. Then successive iterations of calculations were carried out with the new zeta potential, thus affecting the particle hydration and size until convergence was achieved when ζ_k values obtained from two successive iterations became stable. We observed that the ICPR phenomenon had an important effect on the pH_k^* mainly when peptide oligomerization occurred increasing P_k and X_k. This phenomenon was associated with the range of high zeta potentials causing a substantial shift of pH_k^* value toward the particle pI. The numerical procedure to correct global properties due to ICPR effects used fixed values of μ_{pk}^{exp} and Ω_k as input data; the former was an experimental data while the latter was provided by the corresponding PLLCEM code, which could sample spherical or aspherical particles for different hydration states within the physical limits allowed (see numerical scheme in the Supporting Information). Here in particular we place emphasis on the aspherical particle case at minimum hydration, which is more compatible with the beta sheet formation of Aβ peptides. In fact our calculations indicated that the spherical particle case was rather unexpected due to the high particle hydration required to meet the physical conditions for this shape (Section 3). For instance Supporting Information Tables S2 and S4 show that to satisfy the spherical shape, δ_k values of the order 10 are required when $k = 20$, while the aspherical case counterpart gives a value around 0.4. At the extreme of very high unexpected values of δ_k, the shifts of pH_k^* almost disappeared (Supporting Information Fig. S1).

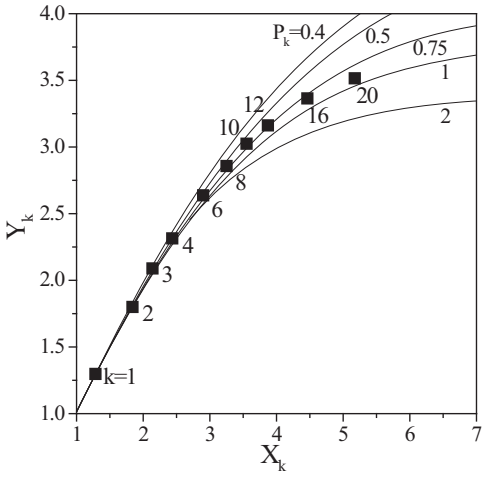

Figure 1. Numerical results (■) of dimensionless electrophoretic mobility $Y_k = 3\mu_{pk}^{exp}\eta_s e/2\Omega_k \epsilon k_B T$ as a function of dimensionless zeta potential $X_k = e\zeta_k/k_B T$ parametrically with the dimensionless Stokes hydrodynamic radius $P_k = \kappa a_{HK}$ for k = 1–20, at 20°C when pH 7.79 and I = 6 mM. Full lines are numerical results reported in [52, 54].

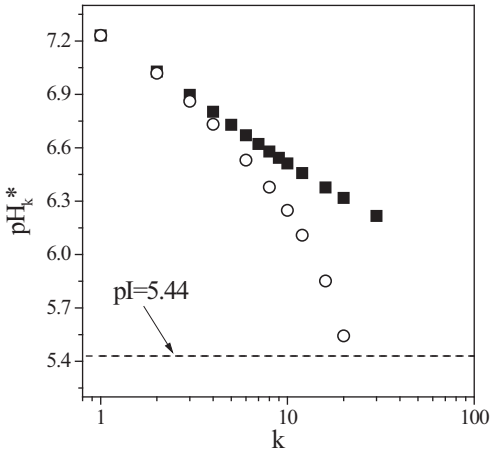

Figure 2. Near molecule pH (designated pH_k^*) of monomer (k = 1) and oligomers (k > 1) of Aβ(1-42) as a function of the oligomerization number k at 20°C when pH 7.79 and I = 6 mM. Symbol (■) indicates calculations where ICPR effects were neglected. Symbol (○) refers to calculations where ICPR effects are considered. Dashed line indicates $pH_k^* = pI$ valid for any *k* value. Aspherical particles sampling conformations with $\Omega_k \neq 1$ and $H_{dk} = 0$ are considered.

3 Results and discussion

Figure 1 shows numerical predictions of Y_k versus X_k of Aβ(1-42) monomer (k = 1) and its oligomers (k = 2-20) when the PLLCEM includes the correction of the zeta potential due to the ICPR phenomenon. From this figure it is clear that these effects start to be significant for around k > 5, where results diverge from the asymptotic straight line $Y_k = Y_k(X_k, P_k)$ found for $X_k < 3$ and $P_k < 3$, satisfying the Henry-Hückel branch. Therefore this straight line is not a solution for the electrophoretic mobilities of oligomers with high values of k. Further as the oligomerization number increases, a remarkable change of the near molecule pH is observed in Fig. 2. This figure shows that pH_k^* is a decreasing function of k, as predicted by the PLLCEM with and without the consideration of the ICPR phenomenon, when aspherical particles sampling conformations for $\Omega_k \neq 1$ and $H_{dk} = 0$ are considered. These conformations with a significant asphericity ($\Omega_k < 1$) are compatible globally with chain beta-strands assembled into beta-sheet structures as expected (Supporting Information Fig. S2). In this context one may visualize that for high k the relative displacement of positive and negative electrical charge centers due to ICPR cannot be neglected when one needs to estimate the rather high zeta potentials around the translating particle yielding also a significant shift of the pH_k^* towards the pI = 5.44. Further when this phenomenon is neglected, one still visualizes that $pH_k^* \rightarrow pI$, as shown in Fig. 2 and also indicated in our previous works for proteins and peptides at different bulk pHs from either left or right limits of the analyte pI value [26, 60]. Nevertheless, the pH_k^* approaches the pI less sharply for increasing k, thus validating comments

in Section 2.2.3 where the need to carry out a correction to the PLLCEM results at high values of k was proposed. It is then evident that the PPCR and IPCR phenomena, as a result of the presence of positive and negative weak ionizing groups in the chain, cannot be neglected in general to estimate the electrostatic state of proteins and peptides, mainly to study pair particle interactions when the particle concentration reaches a critical value. In this regard, some physical conclusions emerge from our previous and present works [31, 32]: (i) both the IPCR and the PPCR phenomena produce shifts of pH_k^* toward the chain pI value, (ii) the PPCR may be considered equivalent to the IPCR when the jointing particles are effectively aggregated (oligomerization occurs on contact) and (iii) as k increases the pH_k^* produced by the IPCR is still lower and closer to the pI than those of the corresponding monomers and previous aggregating pair particles. This systematic lowering of the pH_k^* for increasing k can be associated with the amyloid cascade pathway. Thus when pH_k^* becomes rather close to the pI, the precipitation of the aggregates may be expected for critical peptide concentration and oligomerization number, at which the previous required enhancement of the PPCR phenomenon occurs.

Numerical values of electrokinetic and hydrodynamic global properties of the monomers Aβ(1-40) and Aβ(1-42) peptides ($k = 1$) and their oligomers ($k = 2$ to 20), obtained from the PLLCEM without and with correction due to ICPR phenomenon are presented in the Supporting Information Tables S1 to S6 . From these calculations one observes that the values of electrokinetic global properties of Aβ(1-42) and Aβ(1-40) are quite similar. These results are expected [31] because these peptides differ in two hydrophobic neutral amino acids residues only (Ile and Ala). In this regard, we already showed [31] that one reason for the major propensity to aggregation of Aβ(1-42) was due to the higher repulsive hydration force present in the pair particle interaction potential of the Aβ(1-40). In fact the Aβ(1-42) is less hydrated and more hydrophobic than Aβ(1-40). This last analysis shows that before the IPCR phenomenon occurs in soluble oligomers promoting the precipitation of amyloids beta peptides for high k, a favorable condition involving the imbalance among hydration, electrostatic and dispersion forces must be satisfied to get the particles close enough, thus allowing the switch from interacting pair particles to jointed particles.

Particular results are obtained in the aggregation of two monomers yielding a dimer. Thus, Aβ(1-40) and Aβ(1-42) oligomers present $\Omega_k > 1$ for $k = 2$ only (see Supporting Information Tables S1 and S3 and Fig. S2) indicating that a surface slip occurs between particle and fluid [28]. This result is compatible with the low values of the fractal friction dimensions calculated ($g_{fk} \approx 0.36$ for both peptides) representing a rather compact structure approaching the collapse globule regime [20, 22]. This is consistent with previous studies [61] showing that monomers present the chain region (10-24) associated with either alpha-helix or beta-strand conformations between two beta turns, where the later motif is the one yielding a rather low energy compact dimer forming structurally organized beta-sheets, including also the beta-strand end-terminal region of monomers. In this regard one may speculate here from values of global properties that $k = 2$ involves a rather particular nucleating state of oligomerization. Similar conclusions for $k = 2$ may be obtained from Supporting Information Tables S2 and S4 when the less probable spherical particles are sampled, where less water occluded is required having lower a_{Hk} and g_{fk}, and remarkably with $H_{dk} = H_k - H_{ok} < 0$ because $\Omega_k > 1$ must be reduced to $\Omega_k = 1$.

From our preliminary calculations above, the following rationale concerning the steps leading to oligomerization emerges. By starting from around pH 7.3 to 7.4 and chain pI = 5.44, any increase of monomer concentration from the normal values yields an enhancement of the pH_k^* shift toward the pI via the PPCR phenomenon, increasing the propensity to aggregation of Aβ peptides [31, 32] as long as the hydration and repulsion interaction potentials are less than the dispersion attractive interaction potential to promote "suspension instability" (mainly Aβ(1-42) with lower hydration repulsion force). In this regard, the chain properties required are relatively high average hydrophobic index, low δ_k, H_k and Z_k, as well as the presence of the ICPR phenomenon as k increases [31]. Therefore consecutive oligomerizations (k increases) push further the pH_k^* shift toward the pI value via the amplified IPCR that is increasing even more the propensity to aggregation of the higher oligomers (Supporting Information Figs. S3 and S4). Consequently if a relatively high monomer concentration is maintained in this process, the "amyloid cascade" generating oligomers with higher oligomerization number k is viable. Since this conclusion is obtained from a normal value of bulk pH, one may indicate in addition that any lower pathological pH (typically found in "acidosis processes") may shorten the time required for the pH_k^* to approach the pI value during the steps described above in the amyloidogenic process.

Finally the important role of the IPCR phenomenon for increasing k in the "amyloide cascade" may be visualized simply by comparing the wild effective charge number (classically estimated through the AAS only) and the calculated with and without the ICPR, as illustrated in the Supporting Information Tables S1 to S6 and Figs. S3 and S4.

4 Concluding remarks

The evolution of the near molecule pH generated by the PPCR and IPCR phenomena during the oligomerization of Aβ(1-40) and Aβ(1-42) peptides is one of the relevant mechanisms involved in the amyloidogenic pathway. Simple scaling laws validate the trend of numerical results obtained for electrokinetic and hydrodynamic global properties of Aβ oligomers. Thus the change of the near molecule pH toward the pI for increasing oligomerization number is the central finding in the present work. These results allow one to rationalize consecutive physical stages making physically viable the "amyloid cascade hypothesis" presented in the literature. To arrive at definite conclusions on these mechanisms, more

experimental information is desirable concerning the evaluation of effective electrophoretic mobilities of Aβ peptides and their oligomers at different incubation times in the same BGE as that of the CZE run. These additional results will be useful to expand the study of the slow aggregation kinetic constants and the amyloid pathway as a rate dependent process.

Authors wish to thank the financial aid received from Universidad Nacional del Litoral, Santa Fe, Argentina (*CAI+D-2011*) *and CONICET* (*PIP-112-201101-00060*).

The Authors have declared no conflict of interest.

5 References

[1] El Rassi, Z., *Electrophoresis* 2010, *31*, 174–191.

[2] Kašička, V., *Electrophoresis* 2010, *31*, 122–146.

[3] Kašička, V., *Electrophoresis* 2012, *33*, 48–73.

[4] Selvaraju, S., El Rassi, Z., *Electrophoresis* 2012, *33*, 74–88.

[5] Righetti, P. G., Sebastiano, R., Citterio, A., *Proteomics* 2013, *13*, 325–340.

[6] Kašička, V., *Electrophoresis* 2014, *34*, 69–95.

[7] Šolínová, V., Kašička, V., Koval, D., Hlaváček, J., *Electrophoresis* 2004, *25*, 2299–2308.

[8] Piaggio, M. V., Peirotti, M. B., Deiber, J. A., *Electrophoresis* 2005, *26*, 3232–3246.

[9] Simó, C., González, R., Barbas, C., Cifuentes, A., *Anal. Chem.* 2005, *77*, 7709–7716.

[10] Benavente, F., Balaguer, E., Barbosa, J., Sanz-Nebot, V., *J. Chromatogr. A* 2006, *1117*, 94–102.

[11] Xin, Y., Mitchell, H., Cameron, H., Allison, S. A., *J. Phys. Chem. B* 2006, *110*, 1038–1045.

[12] Piaggio, M. V., Peirotti, M. B., Deiber, J. A., *Electrophoresis* 2006, *27*, 4631–4647.

[13] Piaggio, M. V., Peirotti, M. B., Deiber, J. A., *Electrophoresis* 2007, *28*, 2223–2234.

[14] Šolínová, V., Kašička, V., Sázelová, P., Barth, T., Mikšík, I., *J. Chromatogr. A* 2007, *1155*, 146–153.

[15] Piaggio, M. V., Peirotti, M. B., Deiber, J. A., *Electrophoresis* 2007, *28*, 3658–3673.

[16] Pei, H., Xin, Y., Allison, S. A., *J. Sep. Sci.* 2008, *31*, 555–564.

[17] Peirotti, M. B., Piaggio, M. V., Deiber, J. A., *J. Sep. Sci.* 2008, *31*, 548–554.

[18] Piaggio, M. V., Peirotti, M. B., Deiber, J. A., *Electrophoresis* 2009, *30*, 2328–2336.

[19] Pei, H., Allison, S., *J. Chromatogr. A* 2009, *1216*, 1908–1916.

[20] Piaggio, M. V., Peirotti, M. B., Deiber, J. A., *J. Sep. Sci.* 2010, *33*, 2423–2429.

[21] Allison, S. A., Pei, H., Allen, M., Brown, J., Chang-II, K., Zhen, Y., *J. Sep. Sci.* 2010, *33*, 2439–2446.

[22] Deiber, J. A., Piaggio, M. V., Peirotti, M. B., *Electrophoresis* 2011, *32*, 2779–2787.

[23] Allison, S. A., Perrin, C., Cottet, H., *Electrophoresis* 2011, *32*, 2788–2796.

[24] Wu, H. F., Allison, S. A., Perrin, C., Cottet, H., *J. Sep., Sci.* 2012, *35*, 556–562.

[25] Deiber, J. A., Piaggio, M. V., Peirotti, M. B., *Electrophoresis* 2012, *33*, 990–999.

[26] Deiber, J. A., Piaggio, M. V., Peirotti, M. B., *Electrophoresis* 2013, *34*, 700–707.

[27] Deiber, J. A., Piaggio, M. V., Peirotti, M. B., *Electrophoresis* 2013, *34*, 708–715.

[28] Deiber, J. A., Piaggio, M. V., Peirotti, M. B., *Electrophoresis* 2013, *34*, 2648–2654.

[29] Šolínová, V., Kašička, V., *Electrophoresis* 2013, *34*, 2655–2665.

[30] Catala-Clariana, S., Benavente, F., Gimenez, E., Barbosa, J., Sanz-Nebot, V., *Electrophoresis*, 2013, *34*, 1886–1894.

[31] Deiber, J. A., Piaggio, M. V., Peirotti, M. B., *J. Sep. Sci.* 2014, *37*, 2618–2624.

[32] Deiber, J. A., Peirotti, M. B., Piaggio M. V., *Electrophoresis* 2015, *36*, 805–812.

[33] Barroso, A., Gimenez, E., Benavente, F., Barbosa, J., Sanz-Nebot, V., *Anal. Chim. Acta* 2015, *854*, 169–177.

[34] Dong, S., Duan, Y., Hu, Y., Zhao, Z., *Translational Neurodegeneration* 2012, *1*, 18–30.

[35] Blennow, K., Hampel, H., Weiner, M., Zetterberg, H., *Nat. Rev. Neurol.* 2010, *6*, 131–144.

[36] Selkoe, D. J., *Cold Spring Harb. Perspect. Biol.* 2011, *3*: a004457.

[37] Masters, C. L., Selkoe, D. J., *Cold Spring Harb. Perspect. Med.* 2012, *2*: a006262.

[38] Cecchini, M., Curcio, R., Pappalardo, M., Melki, R., Caflisch, A., *J. Mol. Biol.* 2006, *357*, 1306–1321.

[39] Yan, Y., Wang, Ch., *J. Mol. Biol.* 2006, *364*, 853–862.

[40] Pauwels, K., Williams, T. L., Morris, K. L., Jonckheere, W., Vandersteen, A., Kelly, G., Schymkowitz, J., Rousseau, F., Pastore, A., Serpell, L. C., Broersen, K., *J. Biol. Chem.* 2012, *287*, 5650–5660.

[41] Verpillot, R., Otto, M., Klafki, H., Taverna, M., *J. Chromatogr. A* 2008, *1214*, 157–164.

[42] Sabella, S., Quaglia, M., Lanni, C., Racchi, M., Govoni, S., Caccialanza, G., Calligaro, A., Bellotti, V., De Lorenzi, E., *Electrophoresis* 2004, *25*, 3186–3194.

[43] Kato, M., Kinoshita, H., Enokita, M., Hori, Y., Hashimoto, T., Iwatsubo, T., Toyo'oka, T., *Anal. Chem.* 2007, *79*, 4887–4891.

[44] Colombo, R., Carotti, A., Catto, M., Racchi, M., Lanni, C., Verga, L., Caccialanza, G., De Lorenzi, E., *Electrophoresis* 2009, *30*, 1418–1429.

[45] Picou, R. A., Moses, J. P., Wellman, A. D., Kheterpal, I., Gilman, S. D., *Analyst (Cambridge, United Kingdom)* 2010, *135*, 1631–1635.

[46] Picou, R. A., Kheterpal, I., Wellman, A. D., Minnamreddy, M., Ku, G., Gilman, S. D., *J. Chromatogr. B* 2011, *879*, 627–632.

[47] Verpillot, R., Esselmann, H., Mohamadi, M. R., Klafki, H., Poirier, F., Lehnert, S., Otto, M., Wiltfang, J., Viovy, J. L., Taverna, M., *Anal. Chem.* 2011, *83*, 1696–1703.

[48] Pryor, N. E., Moss, M. A., Hestekin, Ch. N., *Int. J. Mol. Sci.* 2012, *13*, 3038–3072.

[49] Pryor, N. E., Moss, M. A., Hestekin, Ch. N., *Electrophoresis* 2014, *35*, 1814–1820.

[50] Brinet, D., Kaffy, J., Oukacine, F., Glumm, S., Ongeri, S., Taverna, M., *Electrophoresis* 2014, *35*, 3302–3309.

[51] von Smoluchowski, M., *Z. Phys. Chem.* 1917, *92*, 129–168.

[52] Russell, W. B., Saville, D. A., Schowalter, W. R., *Colloidal Dispersions*, Cambridge University Press, Cambridge, UK 1989.

[53] Mansfield, S. L., Jayawickrama, D. A., Timmons, J. S., Larive, C. K., *Biochim. Biophys. Acta* 1998, *1382*, 257–265.

[54] O´Brien, R. W., White, L. R., *J. Chem. Soc. Faraday Trans.* 1978, *74*, 1607–1626.

[55] Allison, S. A., *Biophys. Chem.* 2001, *93*, 197–213.

[56] Allison, S. A., Potter, M., McCammon, J. A., *Biophys. J.* 1997, *73*, 133–140.

[57] Allison, S. A., *Macromolecules* 1996, *29*, 7391–7401.

[58] Allison, S. A., Wu, H., Bui, T. M., Dang, L., Huynh, G. H., Nguyen, T., Soegiarto, L., Truong, B. C., *J. Sep. Sci.* 2014, *37*, 2403–2410.

[59] Wang, S., Chen, Y., Chen, P., Liu, K., *Biochem. Eng. J.* 2006, *29*, 129–138.

[60] Deiber, J. A., Piaggio, M. V., Peirotti, M. B., *Electrophoresis* 2014, *35*, 755–761.

[61] Soto, C., Castaño, E. M., Frangione, B., Inestrosa, N. C., *J. Biol. Chem.* 1995, *270*, 3063–3067.

